Polymer 49 (2008) 2099–2106

Contents lists available at ScienceDirect

Polymer

journal homepage: www.elsevier.com/locate/polymer

Co-aggregation process of poly(ethylene oxide)-*b*-polybutadiene/poly(acrylic acid) based on evolution of interpolymer hydrogen bonding in solutions

Yu Bai [a], Wei-Ping Gao [a], Jing-Jing Yan [a], Yu-Guo Ma [a], De-Hai Liang [a], Zi-Chen Li [a], Bing-Yong Han [b], Wan-Tai Yang [b], Er-Qiang Chen [a,*]

[a] *Beijing National Laboratory for Molecular Sciences, Department of Polymer Science and Engineering and the Key Laboratory of Polymer Chemistry and Physics of the Ministry of Education, College of Chemistry and Molecular Engineering, Peking University, Beijing 100871, China*
[b] *College of Material Science and Engineering, Beijing University of Chemical Technology, Beijing 100029, China*

ARTICLE INFO

Article history:
Received 25 November 2007
Received in revised form 3 March 2008
Accepted 4 March 2008
Available online 12 March 2008

Keywords:
Blend solution
Co-aggregation
Hydrogen-bonded complex

ABSTRACT

The co-aggregation process of a diblock copolymer poly(ethylene oxide)-*block*-polybutadiene (PEO-*b*-PB) and a homopolymer poly(acrylic acid) (PAA) in solutions was studied. The number-average molecular weights of both the PEO and PB blocks are 5100 g/mol; the weight-average molecular weight of PAA is ~2000 g/mol. The co-aggregation was induced by adding a PB selective solvent (i.e., alkane or cycloalkane) into the THF solution of the two polymers, with the processes characterized by turbidity, ^{1}H NMR, dynamic light scattering, and microscopy experiments. During the selective solvent titration, the solution underwent a macro-phase separation that was mainly related to PAA, followed by a micro-phase separation that corresponded to the formation of vesicles with the shell of PB block and the core of PAA/PEO complex. The experimental results indicated that the evolution of interpolymer hydrogen bonding complexation between the PAA and PEO blocks determined the co-aggregation process. The loose and soluble interpolymer complex could be formed at rather low selective solvent content (f). The complexation was enhanced with increasing f, resulting in "redissolving" the PAA-rich domains in the blend solutions. Afterwards, the more compact PAA/PEO complex chemically linked with a soluble PB block acted as the building blocks to form the vesicles at higher f.

1. Introduction

The self-assembly of block copolymers in selective solvents has been extensively studied for decades and many new findings have added to our understanding of this stimulating topic [1–6]. The morphology and structure of the solution assemblies are determined by many factors such as the chemical structure, molecular architecture, composition of copolymer, solution conditions (concentration, temperature, solubility, pH, ionic strength, etc), and assembly process as well. Recently, the co-aggregation of homopolymer/block copolymer and/or different block copolymers in blend solutions has been a subject of interest. In blend solutions, the interactions among different polymers or blocks become crucial, and can pronouncedly influence the solution aggregation behavior. It has been found that the solubilization of homopolymers in block copolymer micelles can lead to various phase separation behaviors, depending on the solubility of homopolymers and block copolymers in solutions [7–9]. At a low fraction, the homopolymer that is miscible with the core-forming blocks can be dissolved in the core of the aggregates formed by the block copolymer [10–13]. In this case, the aggregation number of spherical micelles will increase [13]. Moreover, since the stretching of core-forming blocks will be partially relieved due to the accumulation of a small amount of homopolymer in the core center, the non-spherical morphologies may transform to spherical one [7,8,14]. When the homopolymer fraction exceeds its solubility limit in the micelles, large colloidal aggregates which contain a major fraction of homopolymer are formed [12].

When specific interactions, such as electrostatic interaction [15–22] or hydrogen bonding [23–32], between complementary bonding sites on different polymers or blocks are introduced, the interpolymer complexation can facilitate the co-aggregation in blend solutions. Such a complexation can take place rather fast [32–36]. For example, in toluene that is inert to hydrogen bonding, the complexation between poly(styrene-*co*-4-vinylphenol) and poly(ethyl methacrylate) can occur immediately after the two polymer solutions are mixed [33]. Even in THF that is a proton–acceptor solvent, the interpolymer hydrogen bonding can complete within

* Corresponding author. Tel./fax: +86 010 62753370.
E-mail address: eqchen@pku.edu.cn (E.-Q. Chen).

0032-3861/$ – see front matter © 2008 Elsevier Ltd. All rights reserved.
doi:10.1016/j.polymer.2008.03.015

1–2 ms [32]. As the resultant interpolymer complex is very different from the original polymer chains, the aggregation of the preformed complex may generate different types of aggregates in terms of morphology and structure [23–26]. For example, we have recently demonstrated that while a pure poly(ethylene oxide)-*block*-polybutadiene (PEO-*b*-PB) itself forms spherical micelles in a mixed solvent of THF/*n*-dodecane, a co-aggregation based on interpolymer hydrogen bonding between the PEO block and a homopolymer of poly(acrylic acid) (PAA) can produce vesicles with the PAA/PEO complex as the core and the soluble PB as the shell in the solvent mixture when dodecane content is sufficiently high [37].

To induce the PEO-*b*-PB/PAA vesicle formation, we used a titration method, namely, the two polymers were firstly dissolved in THF, a common solvent, followed by a stepwise addition of dodecane which is only selective for the PB block. In general, the addition of dodecane can progressively weaken the hydrogen bonding between THF and PAA; meanwhile, the interpolymer hydrogen bonding between PAA and PEO will develop, which eventually leads to PAA/PEO complex forming the cores of the vesicles. To better understand the co-aggregation mechanism, the present work is concerned with when the interpolymer complexation will take place during the titration and how the evolution of the complexation will affect the co-aggregation pathway. We found that a macro- and a micro-phase separation occurred sequentially upon titration, wherein the macro-phase separation was mainly related to the PAA homopolymer, and the micro-phase separation corresponded to the vesicle formation. Our ^{1}H NMR experimental results suggested that the loose complex of PAA/PEO-*b*-PB formed only when a small amount of the selective solvent was added. The interpolymer complexation was continuously promoted when the solvent property became more selective, and this made the PAA-rich domains "redissolve" in solution. Afterwards, the soluble complex would act as the building blocks to form the vesicles. Dynamic light scattering (DLS) and transmission electron microscopy (TEM) experiments confirmed that the vesicular structure was the most stable in the solvent mixture with high selective solvent content.

2. Experimental section

2.1. Materials and sample preparation

The detailed synthetic procedure and the chemical characterization of PEO-*b*-PB were reported elsewhere [38]. The diblock copolymer possesses a number-average molecular weight (M_n, measured by ^{1}H NMR, Bruker ARX400 spectrometer) of 5100 g/mol for both the PEO and the PB blocks, and its polydispersity (M_w/M_n, measured by GPC, Waters 150) is 1.06. PAA with a weight-average molecular weight (M_w) of ~2000 g/mol was purchased from Aldrich and was used as received.

The PEO-*b*-PB and PAA polymers were first dissolved in THF with an initial diblock concentration (C_0) of 2.5 mg/mL and a weight ratio of PAA to PEO-*b*-PB (W_A/W_{EB}) of 2. Under a moderate mechanical stirring, alkane or cycloalkane as the selective solvent for PB was then gradually dropped into the THF solution until a desired selective solvent content (*f*, volume fraction of the solvent mixture) was reached. For comparison, we also added alkane or cycloalkane to the THF solutions of the pure PAA and PEO-*b*-PB at the matching concentrations.

2.2. Characterization

The selective solvent titration processes were monitored by turbidity measurement and ^{1}H NMR experiment 10 min after the addition of the selective solvent. Using a Cary 1E UV–vis Spectrometer, the turbidity was measured at a wavelength of 650 nm where the absorptions were the lowest for the polymers, solvents, and aggregate solutions, and the solvents were used as the reference. The ^{1}H NMR spectra of the sample in deuterated solvents (THF-d_8 and cyclohexane-d_{12}) were recorded on a Bruker Advance 400-MHz spectrometer using tetramethylsilane as the internal reference.

Laser light scattering (LS) experiments were performed on a Brookhaven Goniometer (BI-200SM) equipped with a BI-TurboCorr Digital Correlator. The vertically polarized laser beam was supplied by a solid-state laser source (Mini L-30, Brookhaven, 30 mW) operating at 636 nm. The THF solution of PAA/PEO-*b*-PB or of pure PEO-*b*-PB was first filtered through Millipore 0.45 μm PTFE filter into a dust-free vial, and then titrated with the filtered selective solvent to a desired *f*. Since the scattered light intensity of the blend solutions would exceed the instrumental limit when the blend solution exhibited rather high turbidity due to a macro-phase separation, the LS experiments were carried out when the turbidity was sufficiently low. The scattering data at 90° were collected in the homodyne mode 10 min after the addition of the selective solvent. For DLS experiments, the time correlation functions were analyzed with a Laplace inversion program CONTIN. The viscosity of the mixed solvent with different compositions was measured using Ubbelohde viscometer, and the refractive index was calculated as the volume-weighted average of solvent components.

The morphology of macro-phase separation of the blend solutions was examined under a phase contrast optical microscopy (PCOM, Olympus BX51) with an Olympus (C-5050ZOOM) digital camera at room temperature. TEM experiments were performed using a JEM-200CX microscope with an accelerating voltage of 120 kV. For the vesicles completely formed at sufficiently high selective solvent content, i.e., at $f \sim 0.9$, the samples for TEM were prepared by directly depositing the blend solutions onto copper grids that were precoated with a thin film of Formvar and then coated with carbon, which were dried freely at ambient conditions followed by drying in vacuum for days. Some of these samples were stained with OsO_4 vapor for 8 min. For $f = 0.5$–0.8, to avoid the morphology change during drying of solutions, we used trace amounts of S_2Cl_2 to crosslink the PB shells and thus fixed the aggregates in solution before the TEM samples were prepared. For the crosslinked samples, no further OsO_4 stain was applied.

3. Results and discussion

In our previous work, we have reported that with titrating *n*-dodecane into the THF solution, PEO-*b*-PB and PAA can co-aggregate into vesicles at dodecane volume fraction *f* of 0.91 [37]. The vesicular membrane is composed of the PAA/PEO complex as the core and the soluble PB as the shell. When using other alkanes or cycloalkanes such as octane, hexane, cyclohexane, etc., we could obtain similar vesicular aggregates. Fig. 1a presents a pristine TEM image of the sample with $W_A/W_{EB} = 2$ obtained in a mixed THF/cyclohexane with the cyclohexane content *f* of 0.91. Although the aggregates stuck together, a higher transmission at the center of aggregates than that around their periphery evidences the vesicular structure. This structure looks clearer after stained by OsO_4 vapor as shown in Fig. 1b, wherein the outer and inner PB layers of the membranes are darker than the cores of PAA/PEO complexes. An overall thickness of the membrane is measured to be 20–30 nm, agreeing with that of the vesicles formed in the mixed THF/dodecane [37].

This multiple-component system is in fact rather complex, wherein the different molecular interactions, e.g., the polymer–solvent interaction, polymer–polymer interaction, especially the hydrogen bonding complexation between PEO block and PAA, are involved. Since the titration procedure progressively turns the medium to be poorer, the interpolymer hydrogen bonding of PEO/PAA will become dominant, and eventually, the PEO/PAA complex forms

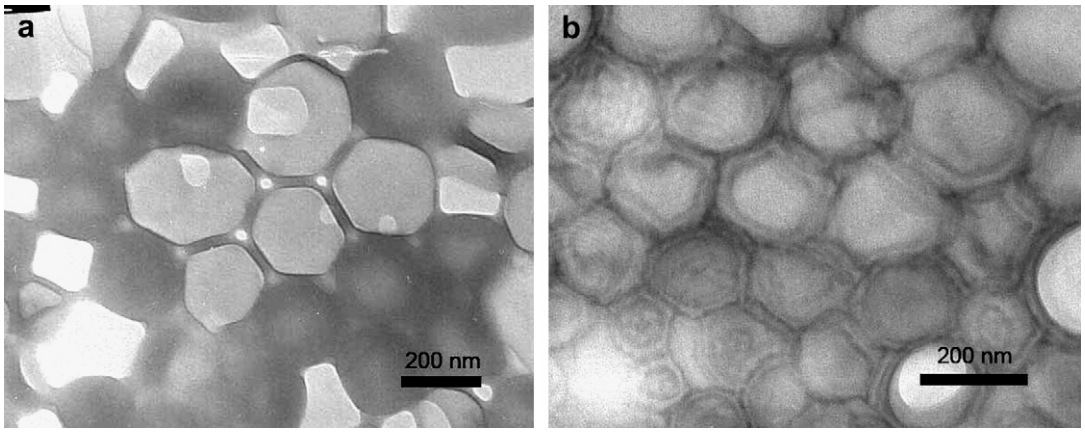

Fig. 1. TEM images of vesicles formed by PAA/PEO-*b*-PB in mixture of cyclohexane/THF at a cyclohexane content *f* of 0.91. The sample shown in (a) was pristine and in (b) was stained with OsO_4.

the cores of the aggregates. To better understand the mechanism of the aggregation, we monitored the whole titration process. Fig. 2 describes the change in turbidity of the PEO-*b*-PB/PAA blend solutions with the selective solvent content *f* of dodecane at 35 °C and of cyclohexane at 25 °C. As the titration diluted the solutions, the turbidity data plotted in Fig. 2 are normalized by the polymer concentration at each *f*. For both the selective solvents used, the turbidity exhibits a process of increase–decrease–increase with *f*. Upon adding dodecane, the turbidity increases dramatically when *f* exceeds 0.17 and reaches a maximum at *f* around 0.23. Afterwards, the turbidity rapidly decreases, followed by a second increase started at $f = \sim 0.37$. When using cyclohexane as the selective solvent, similar phenomenon is observed. Compared with dodecane, cyclohexane is less selective and thus the onset of turbidity rise shifts to a higher *f*. The turbidity firstly increases at $f = 0.22$, arrives a peak at $f = \sim 0.37$, followed by a drop-down and a second increase after $f = 0.5$.

The increase–decrease–increase of turbidity in Fig. 2 indicates a possible two-step phase separation in the blend solution during the titration. Since the first turbidity increase reaches a much higher value than the second one, we consider that this is reminiscent of the "anomalous" micellization in the solution self-assembly of block copolymers [2,10,39–41]. The anomalous micellization of

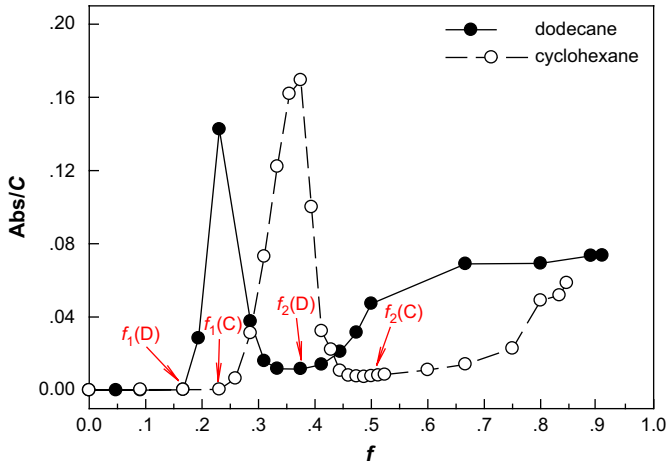

Fig. 2. Turbidity of the PAA/PEO-*b*-PB solution as a function of selective solvent content *f*. The measurements were carried out at 35 °C for dodecane (D) and at 25 °C for cyclohexane (C). The C_0 of PEO-*b*-PB in THF was 2.5 mg/mL and the W_A/W_{EB} was 2. The turbidity data were normalized by the polymer concentration *C*. The red arrows indicate the onsets of the first (f_1) and second (f_2) increase of turbidity (for interpretation of the references to colour in this figure legend, the reader is referred to the web version of this article).

diblock copolymer can arise from the presence of insoluble homopolymers in the solution [39,40]. According to the recent work by Lodge et al. [40], the incipient phase separation of small amount of homopolymers in a block copolymer solution can occur over a modest temperature interval above the critical micelle temperature (CMT) of the copolymer, resulting in the anomalous micelles which can give an unusually large scattering intensity. When the temperature is lowered to the CMT, the scattering intensity of the solution rapidly decreases, followed by an increase that corresponds to the micelle formation that contains the homopolymer in micellar cores. For the system we studied, the Flory–Huggins interaction parameters (χ) of PB/THF and PEO/THF were calculated to be 0.40 and 0.42, respectively [42]. Since PAA may form hydrogen bonding interaction with the proton-acceptor solvent of THF, the χ value of PAA/THF shall also be smaller than 0.5. Adding a selective solvent in THF can increase χ, of which the effect is similar to that of lowering temperature for a UCST solution. We suspect that the first turbidity increase is associated with a macro-phase separation mainly caused by the homopolymer PAA, and the second turbidity increase is related to the morphology evolution towards the vesicles.

We determined the critical dodecane and cyclohexane contents where the precipitation [f^*(PAA)] or micellization [f^*(PEO-*b*-PB)] took place upon adding the selective solvent into the THF solutions of pure PAA and PEO-*b*-PB. The solution concentrations were chosen to be identical to those of the blend solutions. Since the micelle solutions of PEO-*b*-PB remained almost transparent, the f^*(PEO-*b*-PB) was measured by static LS method. Table 1 summarizes the results, which also includes the onsets of the two sequential turbidity increases, f_1 and f_2, obtained from Fig. 2 for a comparison. Obviously, the values of f_1 agree with that of f^*(PAA), implying that the first turbidity increase of the blend solution is indeed due to the phase separation of PAA in solution. Fig. 3 shows a PCOM image of the phase separation morphology of the blend solution with a dodecane content *f* of 0.23, wherein both individual particles and particle clusters are found. The particles were quite mobile

Table 1
The critical selective solvent or nonsolvent contents of phase separation of the pure PAA, PEO-*b*-PB solution, and PAA/PEO-*b*-PB blend solution

Selective solvent	f^*(PAA)[a]	f^*(PEO-*b*-PB)[b]	f_1[c]	f_2[c]
Dodecane	0.17	0.63	0.17	0.37
Cyclohexane	0.23	0.76	0.23	0.50

[a] f^*(PAA) was measured by turbidity experiment.
[b] f^*(PEO-*b*-PB) was measured by static LS.
[c] f_1 and f_2 are the onsets of the first and second turbidity increase of PAA/PEO-*b*-PB blend solutions during selective solvent titration (see Fig. 2).

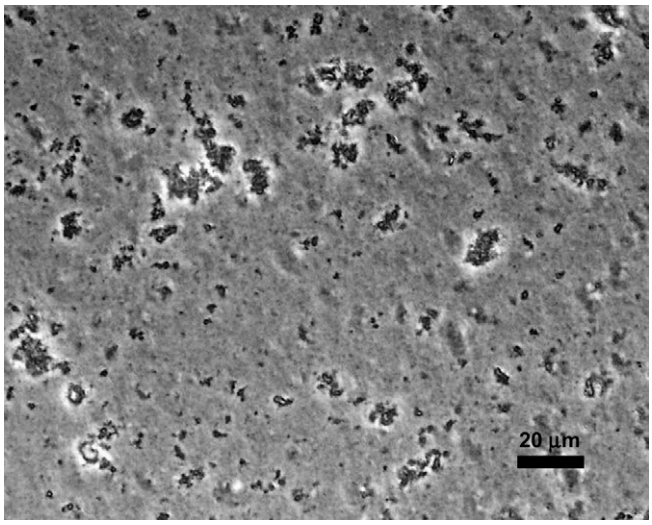

Fig. 3. PCOM image of macro-phase separation morphology of the PAA/PEO-*b*-PB blend solution at the dodecane content $f = 0.23$.

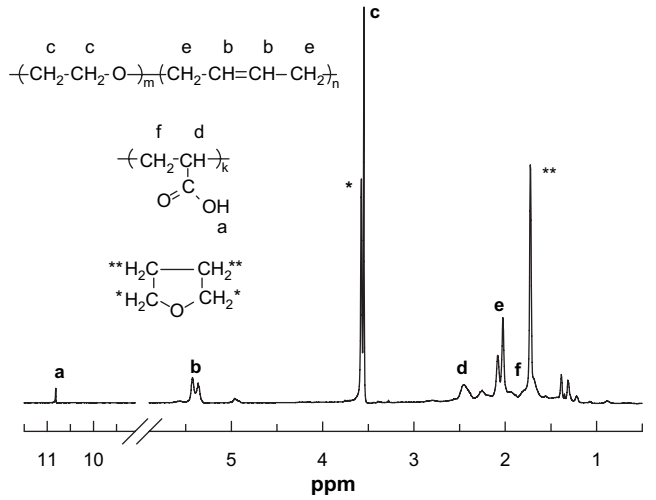

Fig. 4. ^{1}H NMR spectrum of PAA/PEO-*b*-PB in THF-d_8 measured at 25 °C. The peaks of the residual nondeuterated THF is marked with * and **.

under PCOM, and could stick together when they impinged. However, the morphology of particle clusters could be retained for a reasonably long observation time. This means that the particle coarsening is rather slow. We assume that the particles represent the PAA-rich phase with the interface emulsified by PEO-*b*-PB.

We found that for the blend solution with the f of dodecane exceeded 0.3, where the solution turbidity passed its maximum, no particles in micron size could be observed under PCOM. Therefore, the sharp decrease of turbidity in a rather narrow f range is associated with "redissolving" the PAA-rich particles in solution. The subsequent turbidity increase should be related to the second aggregation process which eventually results in the vesicles. It is worth noting that the second aggregation starts at a remarkably lower selective solvent content (f_2 in Table 1) than f^*(PEO-*b*-PB) where the pure PEO-*b*-PB undergoes micellization. Both the "redissolving" of PAA-rich domains and the earlier occurrence of the second aggregation suggest that the interpolymer hydrogen bonding between the PAA and the PEO blocks plays crucial role in our blend solutions, unlike other block copolymer/homopolymer solutions without specific interactions.

To reveal when and how the PAA/PEO interaction occurs, we used ^{1}H NMR experiments to trace the co-aggregation process of the blend solution titrated by cyclohexane at 25 °C. Fig. 4 shows the ^{1}H NMR spectrum of the sample in pure THF-d_8 and the assignments of resonance peaks. To illustrate more clearly the proton resonances varying with the progressive addition of cyclohexane, Fig. 5a–c presents the enlarged NMR spectra of three selected chemical shift ranges, i.e., δ of 10.2–10.6 ppm, 3.4–3.7 ppm, and 5.1–5.7 ppm, which correspond to the protons from the carboxylic acid of PAA, PEO, and PB, respectively. In Fig. 5b, the resonance at 3.58 ppm belongs to the protons from undeuterated THF. This peak locates at the same chemical shift despite the solvent composition, and moreover, its integrated intensity decreases almost linearly with the increased volume ratio of cyclohexane to THF. Therefore, we use this THF proton resonance peak as a reference to correct the dilution effect on the spectral intensity caused by titration.

For the carboxylic acid of PAA, a careful examination could reveal a very broad and weak resonance ranged from δ of 10.5–11.5 ppm at f below 0.28, which is usually ascribed to the existence of loosely bound aggregates of PAA in solution. It became completely undetectable afterward, due to the PAA aggregation development with increasing f. The sharp peak observed in Fig. 5a is suggested to be possibly related to the free carboxylic acid ends of PAA [43]. This peak takes on a notable upfield shift, of which the chemical shift is plotted as a function of f in Fig. 6. For comparison, we have examined ^{1}H NMR of the THF solution of pure PAA titrated with cyclohexane, wherein the sharp resonance at ~10.7 ppm could also be clearly identified until the PAA precipitates fully solidified at f above 0.6. As seen in Fig. 6, the protons from free carboxylic acid ends of both pure PAA and the blend solution share almost the same chemical shift at each f. This suggests that the observed upfield shift is most likely caused by the change in the solvent property. THF as a proton-acceptor solvent can interact with PAA via hydrogen bonding. When the THF content is reduced, the THF molecules surrounding PAA will be replaced by or exchanged with cyclohexane. The protons of the free carboxylic acid will therefore be subjected to an increase of the electronic shielding effect [44]. For the blend solution, weakening the THF/PAA interaction due to the cyclohexane titration certainly facilitates the complexation between PAA and PEO segments and finally, this interaction overwhelms the hydrogen bonding between PAA and THF. The peak undergoes not only a more pronounced upfield shift but also a broadening after $f = 0.6$. This indicates that the interpolymer hydrogen bonding is further developed and more carboxylic acid ends lose their mobility.

The more direct evidence for the PAA/PEO complexation comes from the resonance peak of PEO protons as shown in Fig. 5b. To quantitatively describe the resonance varying with f, we performed careful deconvolution of the peaks and calculated integrated peak intensity ratio of PEO to THF (I_{PEO}/I_{THF}) (see Fig. 7). The value of I_{PEO}/I_{THF} is 1.23 for the pure THF-d_8 solution. However, after adding a small amount of cyclohexane, the ratio drops to 0.96 at $f = 0.17$ where the blend solution remained clear and transparent. This observation suggests that some PEO segments can interact with PAA via interpolymer hydrogen bonding at rather low f, and thus partially lose their mobility in solution. Consequently, the PEO-*b*-PB molecules can be "dragged" in the macrophase separation, which is mainly due to PAA, at the early stage of titration.

The tendency of the I_{PEO}/I_{THF} with f is largely coincident with that observed in turbidity experiment. In Fig. 2, the turbidity starts to rise at the cyclohexane content $f = 0.23$, and reaches its maximum at $f = 0.37$. Accordingly, our NMR measurement shows that the I_{PEO}/I_{THF} continuously decreases to a local minimum at $f = 0.38$ (see Fig. 7), inferring the further development of the PAA/PEO hydrogen bonding. We consider that this gradually enhanced

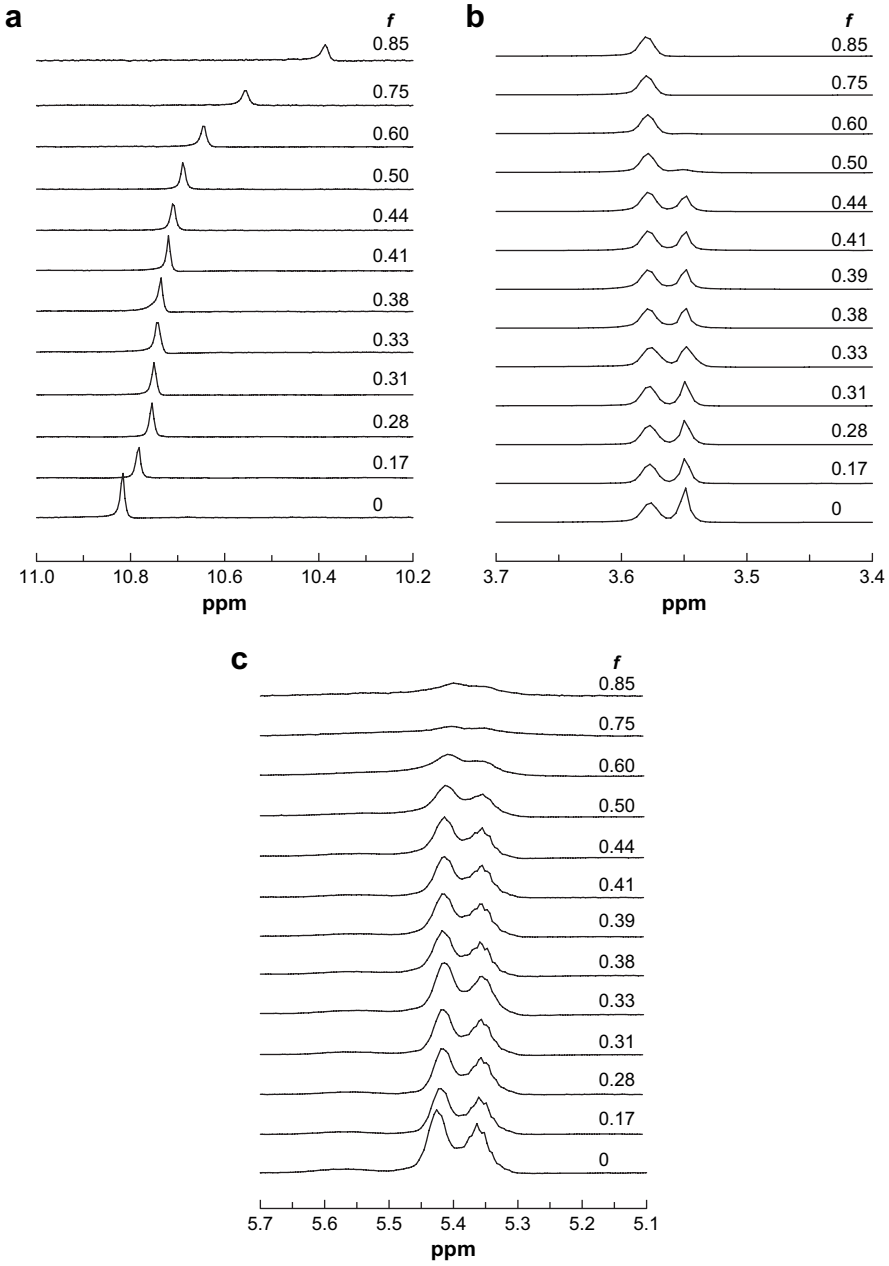

Fig. 5. Sets of ^{1}H NMR spectra of PAA/PEO-*b*-PB in the mixture of THF-d_8 and cyclohexane-d_{12} at various *f*s: (a) PAA, –COOH; (b) PEO, –CH_2–; (c) PB, –CH=CH–.

interpolymer interaction is responsible for the breakdown of the PAA-rich particles. Corresponding to the drastic decrease of turbidity, the I_{PEO}/I_{THF} slightly increases when f increases from 0.38 to 0.41. This implies that while the polymer chains confined in the PAA-rich phase are "redissolved" into solution, part of the PEO segments recover their mobility to a certain extent. At this stage, the PAA/PEO complex may be still loose or ill-defined in structure. Since the complex is chemically linked with a PB block, it shall be more soluble in the solvent mixture in comparison with the complex of homopolymers PAA and PEO with similar loose structures [45,46].

The blend solution possesses the weight ratio of $W_A/W_{EB} = 2$, i.e., the molar ratio of the two repeating units ([AA]/[EO]) of 2.44. Note that the M_n of the PEO block and M_w of PAA are 5100 and 2000 g/mol, respectively, corresponding to the degrees of polymerization of 115 and 27, respectively. Therefore, for the soluble complex, one PEO block may interact with 10 PAA chains [i.e., $2.44 \times (115/27)$] on average. This behavior is similar to that found in the complexation between poly(styrene-*co*-4-vinylphenol) (STVPh) and poly(ethyl methacrylate) (PEMA) when STVPh is in excess [33,36]. Only with this complex structure can the PAA chains avoid macroscopic precipitation after the PAA-rich domains are "redissolved" in solution. Further adding cyclohexane makes the complex become compact. As shown in Fig. 5b, the resonance peak of the proton from PEO dramatically decreases in intensity when f exceeds 0.41, and becomes hardly visible at $f = 0.6$. Using the data in Fig. 7, we may calculate that at $f = 0.5$ only nearly 10% PEO protons $[(I_{PEO}/I_{THF})_{f=0.5}/(I_{PEO}/I_{THF})_{f=0}]$ can be detected by NMR, namely, 90% of the PEO blocks in solution are involved in the PAA/PEO complex. In Fig. 2, the onset of second turbidity increase (f_2) is located at $f = 0.5$, which is an indication of the beginning of the second aggregation. We may conclude that the second aggregation is based on the preformed complex of PAA/PEO-*b*-PB. Compared with the pure PEO-*b*-PB, the complex possesses a lower solubility in the mixed solvent so that its aggregation can take place earlier during titration [47,48].

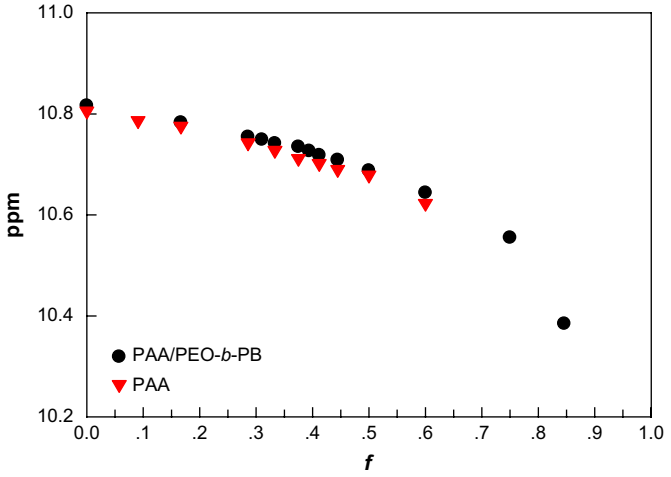

Fig. 6. Chemical shift of the proton on carboxylic acid end of PAA as a function of cyclohexane content *f*.

The second aggregation process is also reflected in NMR spectra of the protons from the PB block (see Fig. 5c). In the selected solvent of PB, the PB protons are observable during the whole titration process. The integrated intensity ratio of the PB resonance peaks at 5.40 and 5.35 ppm to that of THF at 3.58 ppm (I_{PB}/I_{THF}) (see Fig. 7) gradually decreases with increase in *f*. However, a considerable broadening of the two peaks is observed after $f = 0.5$, which is coincident with the second turbidity increase as shown in Fig. 2. The reasons to account for this peak broadening of the shell-forming PB blocks are not fully understood. Probably, the PB segments near the core–shell interface partially lose their mobility [50], particularly when the PB double bonds and the carboxylic acid groups of PAA possess a weak hydrogen bonding interaction [51].

It is of interest to investigate the morphology evolution of the aggregates based on the interpolymer complex. Since the scattered light intensity exceeded the instrumental limit when the solution underwent the macro-phase separation, we utilized DLS to monitor the titration process after the solution turbidity passed its maximum. Fig. 8 illustrates a set of the distributions of the apparent hydrodynamic radius (R_h) measured at an angle of 90° for the blend solution with different dodecane content of *f* at 35 °C. The curves of $f = 0$ and 0.06 are also included for comparison. Before the first turbidity increase, the blend solution exhibits two R_h distributions: the one with $R_h \sim 5$ nm can be assigned to the single molecules in

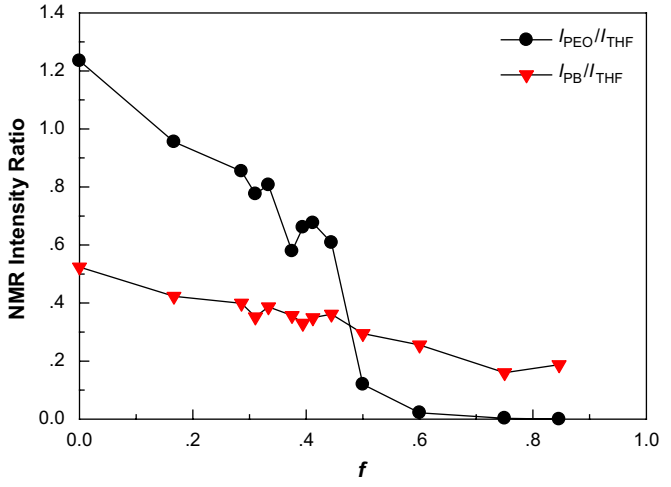

Fig. 7. Integrated intensity ratios of PEO and PB to THF, I_{PEO}/I_{THF} and I_{PB}/I_{THF}, as a function of cyclohexane content *f*. The intensities of I_{PEO} and I_{THF} are obtained from Fig. 5b; the I_{PB} is the sum of the two peaks shown in Fig. 5c.

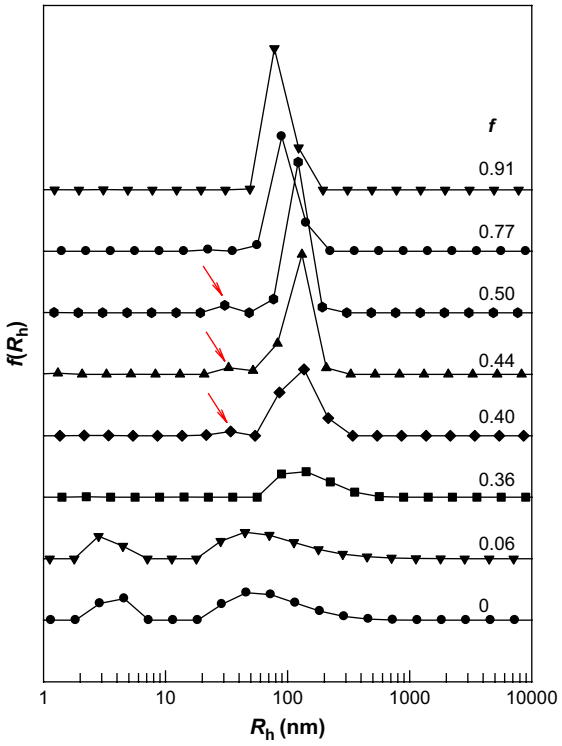

Fig. 8. Set of hydrodynamic radius distributions of PAA/PEO-*b*-PB in THF/dodecane at different values of *f*. The distribution peak of R_h around 30 nm is indicated by the red arrows (for interpretation of the references to colour in this figure legend, the reader is referred to the web version of this article).

the solution; the other with $R_h \sim 50$ nm may come from strongly fluctuating and internally disordered objects of the polymers [49], which is more or less related to the interpolymer interaction between PEO block and PAA in our system. However, only a broad distribution centered at $R_h \sim 100$ nm is observed at $f = 0.36$ right after the turbidity decreases. The disappearance of the peak at $R_h < 10$ nm suggests that most of the PAA and PEO-*b*-PB molecules are incorporated into aggregates. With further increasing *f*, the R_h distribution at ~100 nm gradually narrows until its polydispersity reaches a constant of 0.05 after $f = 0.47$, reflecting the formation of PEO-*b*-PB/PAA vesicles. Interestingly, an additional distribution peaked at R_h of ~30 nm renders on the curves of $0.4 \leq f < 0.77$. Compared to that shown in the turbidity curve of Fig. 2, this *f* range of the dual distribution of R_h corresponds to that of the second increase of turbidity.

The coexistence of the entities with two R_hs can be observed under TEM. Fig. 9a and b show TEM images obtained from the samples at dodecane content *f* of 0.44 and 0.50, respectively. To avoid the aggregate morphology change during solution drying with high THF content, we used trace amounts of S_2Cl_2 to crosslink the PB shells of the aggregates in solution and thus fixed the aggregates before preparing the TEM samples. The large particles shown in the TEM images are the vesicles. However, unlike the vesicles shown in Fig. 1, the center portions of these particles are dark, probably because some residual dodecane remained in the vesicles. As the PB shell was crosslinked, the complete removal of solvent would be inhibited. Careful examination of the TEM images can reveal that the periphery of large particles is more transparent than other parts of the particles, of which the width is of ~14 nm, close to the membrane thickness of 16 nm reported before [37].

In addition to the large dark particles, Fig. 9 also depicts some small particles with less contrast. Their diameter of 20–40 nm agrees with the R_h of 30 nm measured by DLS. One possibility is that these small particles represent the soluble PAA/PEO-*b*-PB

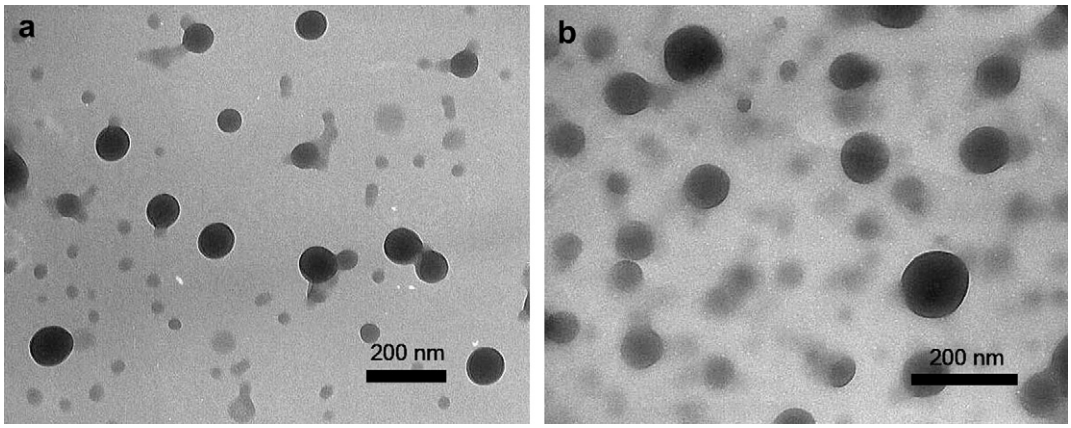

Fig. 9. TEM images of crosslinked samples obtained from the blend solutions with dodecane content f of 0.44 (a) and 0.50 (b).

complexes which are not incorporated into the large aggregates yet. Compared with the individual chains of PAA and PEO-*b*-PB with the R_h of ~5 nm, the complex certainly has an increased size [33–36]. However, although one PEO block may complex with nearly 10 PAA chains, the individual complex size might not reach the R_h of 30 nm because the molecular weights of both the diblock and PAA are low. While the possibility of individual complex cannot be completely excluded, we rather consider that the small particles more likely correspond to spherical micelles of PAA/PEO-*b*-PB. Compared with the spherical micelles formed by the pure PEO-*b*-PB with R_h of 20 nm in the mixed solvent [37], the PAA/PEO-*b*-PB micelles is larger because the PAA chains are accommodated in the cores. This behavior is similar to that observed in diblock copolymer/homopolymer solutions, wherein the micelles diameter is found to increase after loading homopolymer molecules when the spherical micelles of diblock copolymers remain unchanged in the shape [13]. On the other hand, the increased diameter of the PAA/PEO-*b*-PB micelles also reflects that the complexation may extend the PEO block to a certain extent. However, such a micelle structure is less stable than the vesicles when f becomes higher. As shown in Fig. 8, the R_h distribution at ~30 nm completely vanishes at $f > 0.77$. We presume that addition of the selective solvent will finally result in the compact and rigid PAA/PEO complex, and thus favors the vesicle formation [23] more. In this case, the spherical micelles become ruptured, and the newly released interpolymer complexes will be packed into the vesicles.

4. Conclusion

We have studied the co-aggregation process of PEO-*b*-PB and PAA in the blend solutions. With the progressive addition of the selective solvent of the PB block into the THF solution of the two polymers, the solution turbidity exhibited an increase–decrease–increase behavior. Combining the experimental results of morphology observation, ^{1}H NMR, and DLS, we concluded that the first increase in turbidity was related to the macro-phase separation mainly due to PAA, and the second one reflected the formation of vesicles of PEO-*b*-PB/PAA. We found that the evolution of interpolymer hydrogen bonding complexation was crucial for the co-aggregation process. As loose and soluble complex of PAA/PEO could be formed at very low selective solvent content, some PEO-*b*-PB chains would be dragged in the PAA-rich domains when the macro-phase separation occurred. Further adding the selective solvent gradually enhanced interpolymer complexation, leading the PAA-rich domains to be redissolved. Afterwards, the more compact complex that was chemically linked with a soluble PB block in solution started to aggregate, forming both the vesicles and spherical micelles with the PB blocks as the shell and the PAA/PEO complex as the core. However, the spherical micelles vanished finally, indicating that the vesicular structure based on the compact and rigid complex was the most stable at sufficiently high selective solvent content.

Acknowledgement

This work was supported by the National Natural Science Foundation of China (grant no. 20025414, 20374003, and 50573001).

Reference

[1] Halperin A, Tirrell M, Lodge TP. Adv Polym Sci 1992;100:31.
[2] Tuzar Z, Kratochvil P. In: Matijevic E, editor. Surface and colloid science. New York: Plenum; 1993 [chapter 1].
[3] Hamley IW. The physics of block copolymers. Oxford: Oxford University Press; 1998.
[4] Chu B. Langmuir 1995;11:414.
[5] Cameron NS, Corbierre MK, Eisenberg A. Can J Chem 1999;77:1311.
[6] Jain S, Bates FS. Science 2003;300:460.
[7] Zhang LF, Eisenberg A. J Polym Sci Polym Phys Ed 1999;37:1469.
[8] Zhang LF, Shen HW, Eisenberg A. Macromolecules 1997;30:1001.
[9] Lei LC, Gohy JF, Willer N, Zhang JX, Varshney S, Jérôme R. Polymer 2004;48:4375.
[10] Tuzar Z, Bahadur P, Kratochvil P. Makromol Chem 1981;182:1751.
[11] Price C, Stubbersfield RB. Eur Polym J 1987;23:177.
[12] Quintana JR, Salazar RA, Villacampa M, Katime I. Makromol Chem 1993;194:2497.
[13] Quintana JR, Salazar RA, Katime I. J Phys Chem 1995;99:3723.
[14] Zhang LF, Eisenberg A. J Am Chem Soc 1996;118:3168.
[15] Harada A, Kataoka K. Macromolecules 1995;28:5294.
[16] Harada A, Kataoka K. Science 1999;283:65.
[17] Fukushima S, Miyata K, Nishiyama N, Kanayama N, Yamasaki Y, Kataoka K. J Am Chem Soc 2005;127:2810.
[18] Kabanov AV, Bronich TK, Kabanov VA, Yu K, Eisenberg A. J Am Chem Soc 1998;120:9941.
[19] Zhou S, Chu B. Adv Mater 2000;12:545.
[20] Gohy JF, Varshney SK, Jérôme R. Macromolecules 2001;34:3361.
[21] Schrage S, Sigel R, Schlaad H. Macromolecules 2003;36:1417.
[22] Weaver JVM, Armes SP, Liu S. Macromolecules 2003;36:9994.
[23] Antonietti M, Förster S. Adv Mater 2003;15:1323.
[24] Chen D, Jiang M. Acc Chem Res 2005;38:494.
[25] Gohy JF. Adv Polym Sci 2005;90:65.
[26] ten Brinke G, Ruokolainen J, Ikkala O. Adv Polym Sci 2007;207:113.
[27] Liu S, Zhu H, Zhao H, Jiang M, Wu C. Langmuir 2000;16:3712.
[28] Hu J, Liu GJ. Macromolecules 2005;38:8058.
[29] Yan XH, Liu GJ, Hu JW, Willson CG. Macromolecules 2006;39:1906.
[30] Gohy JF, Khousakhoun E, Willet N, Varshney SK, Jérôme R. Macromol Rapid Commun 2004;25:1536.
[31] Lefèvre N, Fustin CA, Varshney SK, Gohy JF. Polymer 2007;45:2306.
[32] Luo SZ, Liu SY, Xu J, Liu H, Zhu ZY, Jiang M, et al. Macromolecules 2006;39:4517.
[33] Zhang YB, Xiang ML, Jiang M, Wu C. Macromolecules 1997;30:2035.
[34] Xiang ML, Jiang M, Zhang YB, Wu C, Feng LX. Macromolecules 1997;30:2313.
[35] Zhang YB, Xiang ML, Jiang M, Wu C. Macromolecules 1997;30:6084.
[36] Xiang ML, Jiang M, Zhang YB, Wu C, Feng LX. Macromolecules 1997;30:5339.
[37] Gao WP, Bai Y, Chen EQ, Li ZC, Han BY, Yang WT, et al. Macromolecules 2006;39:4894.
[38] Gao WP, Bai Y, Chen EQ, Zhou QF. Chin J Polym Sci 2005;23:275.
[39] Tuzar Z, Kratochvil P, Prochazka K, Munk P. Collect Czech Chem Commun 1993;58:2362.

[40] Lodge TP, Bang J, Hanley KJ, Krocak J, Dahlquist S, Sujan B, et al. Langmuir 2003;19:2103.
[41] Zhou ZK, Chu B. Macromolecules 1988;21:2548.
[42] Grulke EA. Solubility parameter values. In: Brandrup J, Immergut EH, editors. Polymer handbook. 3rd ed. New York: Wiley-Interscience; 1989. p. 519 [Section VII].
[43] Cui HG, Chen ZY, Wooley KL, Pochan DJ. Macromolecules 2006;39:6599.
[44] Fujimori K, Trainor GT, Costigan MJ. J Polym Sci Polym Chem Ed 1984;22:2479.
[45] Khutoryanskiy VV, Dubolazov AV, Nurkeeva ZS, Mun GA. Langmuir 2004;20: 3785.
[46] Cohen Y, Prevysh V. Acta Polymerica 1998;49:539.
[47] Saito S, Anghel DF. In: Kwak JCT, editor. Polymer–surfactant systems. New York: Marcel Dekker; 1998. p. 357.
[48] Robb ID, Stevenson P. Langmuir 2000;16:7168.
[49] Edelmann K, Janich M, Hoinkis E, Pyckhout-Hintzen W, Höring S. Macromol Chem Phys 2001;202:1638.
[50] Akiyoshi K, Deguchi S, Moriguchi N, Yamaguchi S, Sunamoto J. Macromolecules 1993;26:3062.
[51] Desiraju GR, Steiner T. The weak hydrogen bond in structural chemistry and biology. Oxford: Oxford University Press; 1999.